Fault Tolerant Permanent Magnet Drives: Operating Under Open-circuit and Short-circuit Switch Faults

Mohammad-Ali Shamsi-Nejad, Babak Nahid-Mobarakeh*, Serge Pierfederici, Farid Meibody-Tabar
Groupe de Recherche en Electrotechnique et Electronique de Nancy (GREEN)
ENSEM-University of Lorraine, 2 av. de la foret de Haye, 54516 Vandoeuvre-Les-Nancy, France

* Corresponding author. E-mail: babak.nahidmobarakeh@univ-lorraine.fr
Received: 15 January 2014; Accepted: 12 February 2014; Published online: 20 February 2014
DOI: 10.14416/j.ijast.2014.01.007

Abstract
A series architecture providing a fault tolerant drive is proposed. The architecture includes one or two DC sources, two voltage source inverters and a PMSM. Three different operating modes are considered: normal mode, open-circuit degraded mode and short-circuit degraded mode. For each case, an adapted torque control strategy is proposed and tested. For the open phase mode, different operating criteria are considered. For short-circuit faults, two solutions are proposed. The proposed strategies are tested on an 8-pole 1 kW PM drive. They allow operating under fault conditions in real-time and their implementation is easy. The experimental results show the effectiveness of the proposed methods.

Keywords*: Fault Tolerant Drives, PMSM, Open Phase Fault, Short-circuit Fault*

1 Introduction

Permanent Magnet Synchronous Machines (PMSM) are well adapted for transportation applications because of their good torque/mass ratio. Obviously, the reliability is an important issue in these applications where the PMSM are supplied by one or two (if available) DC voltage sources through voltage source inverters (VSIs). More, in these applications it is necessary that the system can operate in degraded mode under the presence of almost any fault in one of the electromechanical elements of the energy conversion chain. It is why fault tolerant drives have attracted more and more attention since early nineties [1-23]. A solution to obtain the required level of reliability is to modify the architecture of the drive by replacing each device of low reliability by two or several modular devices of the same nature (in parallel or in series). Voltage source inverters, which have several components, may be considered as the least reliable elements of the system [24]. It is why in some applications, two VSIs are employed in series for supplying the machine (Figure 1). There are two options: supplying by one electrical source with three H-bridges (Figure 1-top) or using two independent electric sources (Figure 1-bottom) in some air and sea transport systems where two independent generators are available. The both cases are called here series architecture.

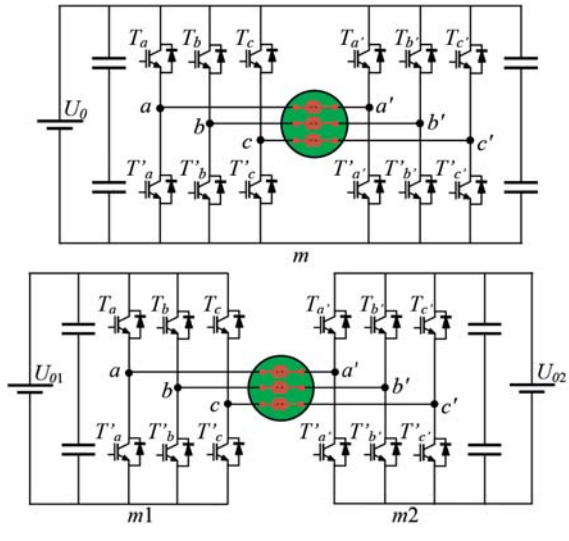

Figure 1: PMSM supplied with one (top) or two (bottom) DC voltage source(s) and two inverters (series architecture).

This paper presents normal and degraded operating modes of this drive. The paper is mainly based on the work published by the authors in [1]. Two degraded modes are considered: T_a in open-circuit and T_a in short-circuit. To improve the torque control performances, proper current control strategies are presented for degraded modes.

There are six sections in this paper. The model of the drive with one or two DC sources is given in the next section. Then, the three operating modes are studied in detail in three sections. The last section concludes the paper.

2 Drive Model and Experimental Set-up

2.1 *Model*

From Figure 1-top, the phase voltages can be written as follows:

$$\begin{bmatrix} v_a \\ v_b \\ v_c \end{bmatrix} = \begin{bmatrix} v_{am} \\ v_{bm} \\ v_{cm} \end{bmatrix} - \begin{bmatrix} v_{a'm} \\ v_{b'm} \\ v_{c'm} \end{bmatrix} = U_0 \cdot \begin{bmatrix} C_a - C_{a'} \\ C_b - C_{b'} \\ C_c - C_{c'} \end{bmatrix} \quad (1)$$

where C_a denotes the "conduction state" of the whole switch containing T_a and its parallel diode together (1 = conducting, 0 = blocking). Then, the machine electric model is the following:

$$\begin{bmatrix} v_a \\ v_b \\ v_c \end{bmatrix} = R_s \cdot \begin{bmatrix} i_a \\ i_b \\ i_c \end{bmatrix} + L_s \cdot \frac{d}{dt} \begin{bmatrix} i_a \\ i_b \\ i_c \end{bmatrix} + \begin{bmatrix} e_a \\ e_b \\ e_c \end{bmatrix} \quad (2)$$

with e_a and i_a as respectively the back-EMF and the current of the phase *a*.

For the architecture shown in Figure 1-bottom, we have $i_a + i_b + i_c = 0$. So, it yields

$$\begin{bmatrix} v_a \\ v_b \\ v_c \end{bmatrix} = T_{33} \cdot \left(\begin{bmatrix} v_{am1} \\ v_{bm1} \\ v_{cm1} \end{bmatrix} - \begin{bmatrix} v_{a'm2} \\ v_{b'm2} \\ v_{c'm2} \end{bmatrix} + \begin{bmatrix} v_{m1m2} \\ v_{m1m2} \\ v_{m1m2} \end{bmatrix} \right) \quad (3)$$

which gives:

$$\begin{bmatrix} v_a \\ v_b \\ v_c \end{bmatrix} = U_{01} T_{33} \cdot \begin{bmatrix} C_a \\ C_b \\ C_c \end{bmatrix} - U_{02} T_{33} \cdot \begin{bmatrix} C_{a'} \\ C_{b'} \\ C_{c'} \end{bmatrix} \quad (4)$$

with:

$$T_{33} = \frac{1}{3} \begin{bmatrix} 2 & -1 & -1 \\ -1 & 2 & -1 \\ -1 & -1 & 2 \end{bmatrix} \quad (5)$$

Three cases are considered in this paper: normal operating, T'_a in open-circuit and T'_a in short-circuit. For each case, the corresponding torque control strategy is studied. For this study, the back-EMF is supposed sinusoidal as follows:

$$\begin{cases} e_a = -\sqrt{\frac{2}{3}} \Psi_f P \Omega \sin(\theta) = -k\Omega \sin(\theta) \\ e_b = -\sqrt{\frac{2}{3}} \Psi_f P \Omega \sin\left(\theta - \frac{2\pi}{3}\right) = -k\Omega \sin\left(\theta - \frac{2\pi}{3}\right) \\ e_c = -\sqrt{\frac{2}{3}} \Psi_f P \Omega \sin\left(\theta + \frac{2\pi}{3}\right) = -k\Omega \sin\left(\theta + \frac{2\pi}{3}\right) \end{cases} \quad (6)$$

It is known that the motor torque expression is the following:

$$\Gamma_m = \frac{e_a i_a + e_b i_b + e_c i_c}{\Omega} \quad (7)$$

Therefore, the torque control strategy consists in determining the references of the phase currents. This can be done in the physical *abc* frame for each studied case, as well as in a rotating synchronous frame (*dq* frame).

2.2 *Experimental test-bed*

The experimental set-up is shown in Figure 2 and its parameters are given in Table 1. It includes an electric machine (on the right of the picture) supplied by two inverters (on the left of the picture) and controlled by a digital control card (on the top of the picture).

Table 1: System Parameters

no. of poles	8
Rated output	1 *kW*
DC-bus voltage	200 *V*
Switching frequency	10 *kHz*
Rated speed	1800 *rpm*
Rated torque	5.8 *Nm*
Stator resistance	0.5 Ω
Stator inductance	3.1 *mH*
Torque constant	24×10^{-3} *kg.m²/s*
Inertia constant	3×10^{-3} *kg.m²*

Figure 2: Experimental set-up at GREEN, Nancy, France.

The machine is a permanent magnet synchronous one. Two IGBT based voltage source inverters supply the machine. The drive is controlled by a dSPACE digital control card (DS1005) whose sampling period is 100 μs. It sends PWM commands to an interface card (SKHI22) and then to IGBTs. The switching frequency is fixed to 10 *kHz*. The DC source voltage is set to 200 *V*. The load is a PM synchronous generator supplying a variable resistance.

3 Normal Operating Mode

This mode is studied to provide a comparison base with faulty modes. To get a non pulsating motor torque in normal operating mode, it is sufficient to have balanced sinusoidal phase currents:

$$\begin{cases} i_a = -I_m \sin(\theta) \\ i_b = -I_m \sin(\theta - 2\pi/3) \\ i_c = -I_m \sin(\theta + 2\pi/3) \end{cases} \quad (8)$$

Then, from (6) and (7), the motor torque is

$$\Gamma_m = \frac{3}{2} k I_m \quad (9)$$

As common, a synchronous rotating frame (*dq*) can be used to make it easier to design the current controllers and to get more robust and efficient current loops. Park transformation is used here:

$$\begin{bmatrix} x_d \\ x_q \end{bmatrix} = P(-\theta) \cdot T_{32}^T \cdot \begin{bmatrix} x_a \\ x_b \\ x_c \end{bmatrix} \quad (10)$$

with:

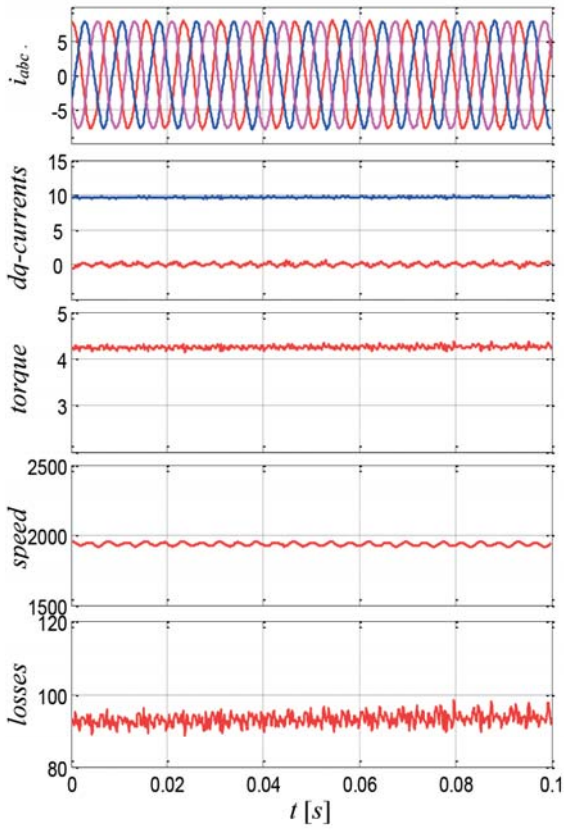

Figure 3: Experimental results under normal operating mode: phase currents (i_{abc}) [A], *dq*-currents [*A*], torque [*Nm*], speed [*rpm*] and losses [*W*].

$$T_{32} = \sqrt{\frac{2}{3}} \begin{bmatrix} 1 & 0 \\ \frac{-1}{2} & \frac{\sqrt{3}}{2} \\ \frac{-1}{2} & \frac{-\sqrt{3}}{2} \end{bmatrix}, \quad P(\theta) = \begin{bmatrix} \cos\theta & -\sin\theta \\ \sin\theta & \cos\theta \end{bmatrix} \quad (11)$$

in which θ is the electrical position of the rotor and $x = v, e, i$. The motor torque expression in this rotating frame is given by:

$$\Gamma_m = \sqrt{3/2} \cdot k \cdot i_q \quad (12)$$

From (12), it is clear that *q*-current should be constant to obtain a constant non pulsating torque.

Experimental results are shown in Figure 3 for the normal operating mode. The motor torque (estimated according to (7)) does not oscillate and *dq*-currents are almost constant. The phase currents (i_a, i_b, i_c) are balanced. The experimental set-up and its parameters are described in Table 1.

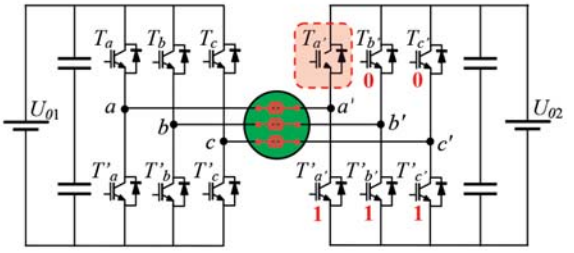

Figure 4: Forming a neutral point under an open-circuit fault (two independent sources).

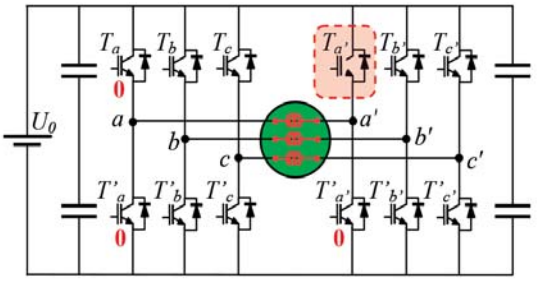

Figure 5: Forcing the current to zero under an open-circuit fault (one source).

Note- To maximize the available voltage for operating at high speed, the conducting state of the corresponding switches in the two inverters are complementary ($C_a = \bar{C}_{a'}$, $C'_a = \bar{C}'_{a'}$, …).

4 Open-circuit Operating Mode

When T'_a is in open-circuit, i_a can no more be controlled. We have to commutate to a degraded mode. Two different strategies may be adopted:

- forming a neutral point by connecting the points *a'*, *b'* and *c'* (Figure 4),
- or forcing i_a to zero (Figure 5).

The former solution is easy to implement. It is particularly well adapted to the architecture in Figure 1-bottom because $i_a + i_b + i_c = 0$. It should be noted that this reduces the available voltage and so the maximum achievable speed.

The latter solution is more suitable for the architecture in Figure 1-top. For forcing i_a to zero, just let's open the other three transistors related to the faulty phase ($T'_{a'}$, T'_a and T_a) as illustrated on Figure 5. Then, the remaining phase currents (i_b and i_c) should be controlled to suppress the resulting pulsating torque due to unbalance. To do that, it is known that the opened phase current should be put, in the opposite sign, to one of the healthy phases. In our case, $-i_{a\,healthy} = +I_m \sin(\theta)$ (see (8)) should be the reference of i_b or i_c in the faulty case. From (6) and (7), it can be easily verified that a non pulsating torque is achieved using this strategy. Here, we choose $i_{c\,faulty} = -i_{a\,healthy}$:

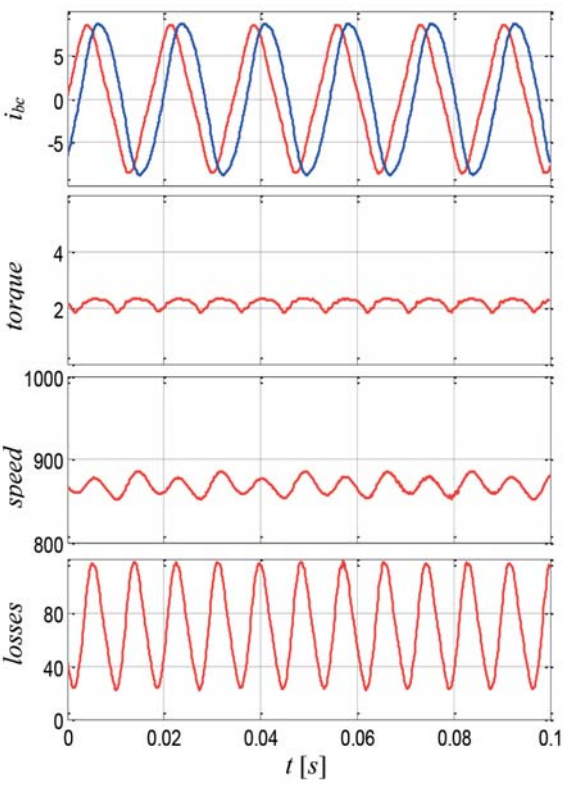

Figure 6: Experimental results under open phase fault using (13): phase currents (i_{bc}) [*A*], torque [*Nm*], speed [*rpm*] and losses [*W*].

$$\begin{cases} i_a = 0 \\ i_b = -I_m \sin(\theta - 2\pi/3) \\ i_c = +I_m \sin(\theta) \end{cases} \tag{13}$$

From (13), (6) and (7), it yields

$$\Gamma_m = \frac{3}{4} k I_m \tag{14}$$

Comparing (14) with (9), it can be concluded that the motor torque under open-phase fault is the half of that in the normal operating mode.

Figure 6 shows experimental results when the

phase *a* is opened and current references in (13) are applied to control the motor torque. As was expected, the motor torque is about 2.1 *Nm* (for 4.2 *Nm* in the normal mode). The pulsating torque is almost suppressed. There is just a small residual pulsating torque because of the limited bandwidth of the current control loops. It should be noted that the current control is realized in the *dq* rotating synchronous frame.

In [1], the authors showed that it is also possible to improve the average torque in the faulty mode if DC sources are electrically connected (Figure 1-top for example). The question is how to change the remaining phase currents (i_b and i_c) in order to suppress the pulsating torque while maximizing the average torque. To do that, consider two independently controlled phase currents i_b and i_c:

$$\begin{cases} i_a = 0 \\ i_b = -I_m \sin(\theta - \beta) \\ i_c = -I'_m \sin(\theta - \gamma) \end{cases} \tag{15}$$

Then, from (6), (7) and (15), the motor torque expression is given in Eq. (16):

$$\begin{aligned} \Gamma_m = {} & kI_m \cdot \sin(\theta - \beta) \cdot \sin(\theta - 2\pi/3) \\ & + kI'_m \cdot \sin(\theta - \gamma) \cdot \sin(\theta + 2\pi/3) \end{aligned} \tag{16}$$

After simplifying, we get:

$$\begin{aligned} \Gamma_m = {} & \frac{kI_m}{2}\left(\cos(2\theta - \beta - 2\pi/3) + \cos(\beta - 2\pi/3)\right) \\ & + \frac{kI'_m}{2}\left(\cos(2\theta - \gamma + 2\pi/3) + \cos(\gamma + 2\pi/3)\right) \end{aligned} \tag{17}$$

Then, to suppress the pulsating torque, we have the following:

$$\begin{cases} I_m = -I'_m \\ \gamma - \beta = \dfrac{4\pi}{3} \end{cases} \tag{18}$$

which leads to the following constant torque:

$$\Gamma_m = \frac{kI_m}{2}\left(\cos(\beta - 2\pi/3) - \cos(\beta)\right) \tag{19}$$

This torque will be maximized if:

$$\beta = \frac{5\pi}{6},\ \gamma = \frac{\pi}{6} \tag{20}$$

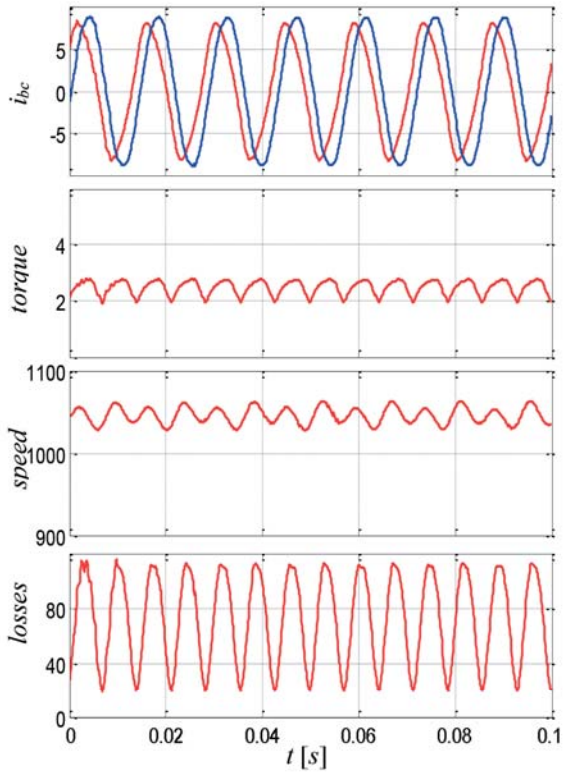

Figure 7: Experimental results under open phase fault using (15): phase currents (i_{bc}) [*A*], torque [*Nm*], speed [*rpm*] and losses [*W*].

Replacing (20) in (19), we obtain the following constant torque under open-phase fault condition:

$$\Gamma_m = \frac{\sqrt{3}}{2} kI_m \tag{21}$$

It is clearly more advantageous to choose i_b and i_c according to (15), (18) and (20), if possible (one common source or two connected sources), because the torque in (21) is 15% greater than that in (14).

Experiments have been performed with an open phase when Eq. (15) is used to fix the remaining phase currents. Their results are shown in Figure 7. It is obvious from the angular speed that the average torque is slightly greater than that in Figure 6.

Instead of maximizing the torque, it is also possible to minimize the losses [1]. To do it, the current vector has to be collinear with the back-EMF vector. This implies:

$$\frac{e_b}{i_b} = \frac{e_c}{i_c} \tag{22}$$

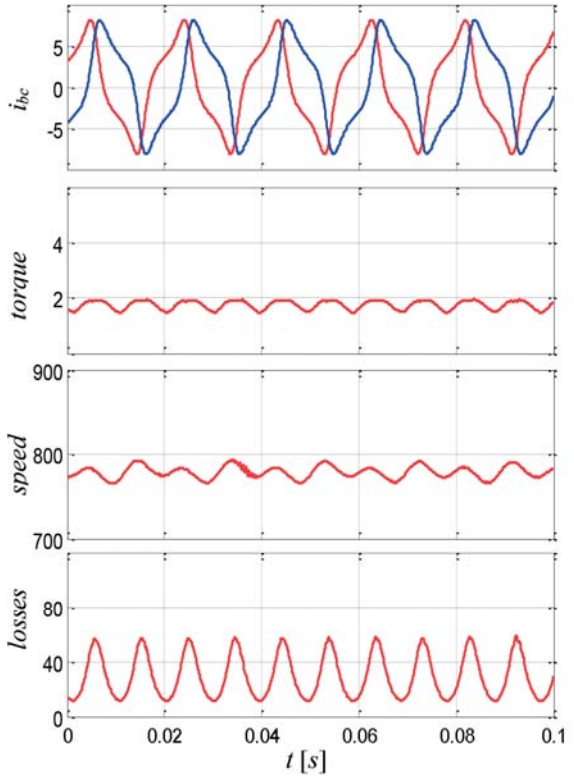

Figure 8: Experimental results under open phase fault using (23): phase currents (i_{bc}) [A], torque [Nm], speed [rpm] and losses [W].

From (22), (6) and (7), it yields

$$\begin{cases} i_b = \dfrac{4}{5}\cdot\dfrac{\sin(\theta-2\pi/3)}{3/2-\sin^2(\theta)}\cdot I_m \\ i_c = \dfrac{4}{5}\cdot\dfrac{\sin(\theta+2\pi/3)}{3/2-\sin^2(\theta)}\cdot I_m \end{cases} \quad (23)$$

Figure 8 depicts experimental results under open phase conditions when healthy phases are set to (23). The machine losses are reduced significantly with respect to the previous control strategies (compare Figure 8 with Figures 6 and 7). The pulsating torque is negligible and the average torque is slightly less than those in Figures 6 and 7. It should be noted that the current references in (23) requires big efforts from the current controllers because of their special shape. The control of the remaining currents is a rotating frame cannot solve this issue.

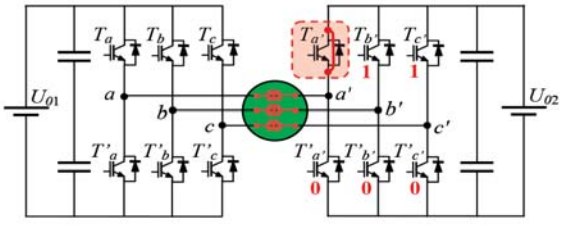

Figure 9: Series architecture with a short-circuit fault (two independent sources).

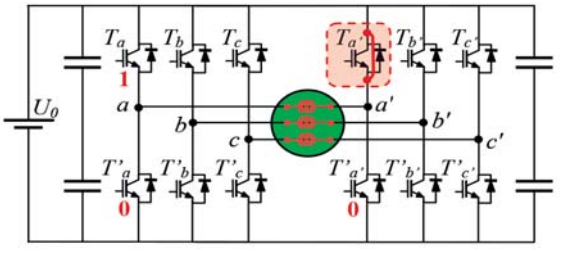

Figure 10: Series architecture with a short-circuit fault (one source).

5 Short-circuit Operating Mode

In the case of a short-circuit fault on T_a, i_a is no more controllable and we have to commutate to a degraded mode. The only solution that we propose here is to form a neutral point by connecting the points *a'*, *b'* and *c'* as shown in Figure 9 [1]. Then, the machine will be controlled with the healthy inverter as a simple three phase machine. It is obvious that the available voltage will reduce with this strategy and the rated speed may not be achieved in the degraded mode.

If there is only one DC source for supplying the both inverters, then the solution consists in short-circuiting the faulty phase by proper command signals (Figure 10). But in this case, the machine should be well studied and designed in order to limit the short-circuit current.

6 Conclusions

A series architecture consisting of one or two DC sources, two voltage source inverters and a PMSM is studied in this paper. The objective is to realize a fault tolerant drive for aerospace applications. Three different operating modes are considered: normal mode, open-circuit degraded mode and short-circuit degraded mode. Different torque control strategies are

studied and compared.

For the open phase mode, according to the number of independent sources, two general strategies are studied. The pulsating torque and the motor losses are minimized under fault conditions. In the case of short-circuit faults, a simple strategy is proposed. For the case of one DC source, it needs some precautions while designing the machine.

The proposed strategies in this paper are effectively applied to a test bench. They allowed operating under fault conditions in real-time and their implementation is easy. The experimental results show the effectiveness of the proposed methods.

References

[1] M.A. Shamsi-Nejad, B. Nahid-Mobarakeh, S. Pierfederici, and F. Meibody-Tabar, "Control Strategies for Fault Tolerant PM Drives Using Series Architecture," in *Proc. VPPC'10*, Sep. 2010, pp. 1-6.

[2] J.R. Fu and T.A. Lipo, "Disturbance-free operation of a multiphase current-regulated motor drive with an open phase," *IEEE Transactions on Industry Applications*, vol. 30(5), pp. 1267-1274, Sep./Oct. 1994.

[3] A. Bouscayrol, B. Davat, B. De Fornel, B. François, J.P. Hautier, F. Meibody-Tabar, and M. Pietrzak-David, "Multi-machine multi-converter systems: applications to electromechanical drives," *EPJ Applied Physics*, vol. 10(2), pp. 131-147, May 2000.

[4] B. Nahid-Mobarakeh, F. Meibody-Tabar, and F.M. Sargos, "A Self-Organizing Intelligent Controller for Speed and Torque Control of a PMSM," in *Proc. IAS'00*, Rome, Oct. 2000, pp. 1283-1290.

[5] R.B. Sepe, B. Fahimi, C. Morrison, and J.M. Miller, "Fault tolerant operation of induction motor drives with automatic controller reconfiguration," in *Proc. IEMDC'01*, Cambridge, 2001, pp. 156-162.

[6] B. Nahid-Mobarakeh, F. Meibody-Tabar, and F.M. Sargos, "Robustness study of a model-based technique for mechanical sensorless PMSM," in *Proc. PESC'01*, Vancouver, 2001, pp. 811-816.

[7] G. Didier, H. Razik, and H. Rezzoug, "On the modeling of induction motor model including the first space harmonics for diagnostics purposes," *ICEM'2002*, Bruges, Jan. 2004.

[8] C.B. Jacobina, R.S. Miranda, M.B. De R. Corrêa, and A.M.N. Lima, "Disturbance-free operation of a six-phase AC motor drive system," in *Proc. PESC'04*, Aachen, Jun. 2004, vol. 2, pp. 925-931.

[9] Dan Sun and Yikang He, "A modified direct torque control for PMSM under inverter fault," in *Proc. ICEMS'05*, 2005, pp. 2473-2473.

[10] A.M. Mendes and A.J. Marques Cardoso, "Fault-Tolerant Operating Strategies Applied to Three-Phase Induction-Motor Drives," *IEEE Transactions on Industrial Electronics*, vol. 53(6), pp. 1807-1817, Dec. 2006.

[11] M.E.H. Benbouzid, D. Diallo, and M. Zeraoulia, "Advanced Fault-Tolerant Control of Induction-Motor Drives for EV/HEV Traction Applications: From Conventional to Modern and Intelligent Control Techniques," *IEEE Transactions on Vehicular Technology*, vol. 56(2), pp. 519-528, March 2007.

[12] O. Wallmark, L. Harnefors, and O. Carlson, "Control Algorithms for a Fault-Tolerant PMSM Drive," *IEEE Transactions on Industrial Electronics*, vol. 54(4), pp. 1973-1980, Aug. 2007.

[13] T. Boileau, B. Nahid-Mobarakeh, and F. Meibody-Tabar, "Back-EMF based detection of stator winding inter-turn fault for PM Synchronous Motor Drives", in *Proc. VPPC'2007*, Arlington, Texas, 2007, pp. 1273-1279.

[14] A. Gaillard, S. Karimi, P. Poure, S. Saadate, and E. Gholipour, "A fault tolerant converter topology for wind energy conversion system with doubly fed induction generator," in *Proc. EPE'07*, Aalborg, 2007.

[15] M.A. Shamsi-Nejad, B. Nahid-Mobarakeh, S. Pierfederici, and F. Meibody-Tabar, "Fault tolerant and minimum loss control of double-star synchronous machines under open phase conditions," *IEEE Transactions on Industrial Electronics*, vol. 55(5), pp. 1956-1965, May 2008.

[16] C. Gerada and K.J. Bradley, "Integrated PM machine design for an aircraft EMA," *IEEE Transactions on Industrial Electronics*, vol. 55(9), pp. 3300-3306, Sep. 2008.

[17] M. Jones, S.N. Vukosavic, and E. Levi, "Parallel-Connected Multiphase Multidrive Systems With

Single Inverter Supply," *IEEE Transactions on Industrial Electronics*, vol. 56(6), pp. 2047-2057, Jun. 2009.

[18] S. Khwan-on, L. de Lillo, L. Empringham, P. Wheeler, C. Gerada, N.M. Othman, O. Jasim, and J. Clare, "Fault tolerant power converter topologies for PMSM drives in aerospace applications," in *Proc. EPE'09*, Barcelona, Sep. 2009.

[19] Hai Lin, Hong Li, Yintao Wang, Mingfeng Li, Peng Wen, and Chunhui Zhang, "On inverter fault-tolerant operation vector control of a PMSM drive," in *Proc. ICIS'09*, 2009, pp. 522-526.

[20] I. Stamenkovic, N. Schofield, N. Milivojevic, M. Krishnamurthy, and A. Emadi, "A novel modular permanent-magnet electric machine design," in *Proc. IECON'09*, Porto, Nov. 2009, pp. 997-1002.

[21] Z. Sun, J. Wang, G.W. Jewell, and D. Howe, "Enhanced Optimal Torque Control of Fault-Tolerant PM Machine Under Flux-Weakening Operation," *IEEE Transactions on Industrial Electronics*, vol. 57(1), pp. 344-353, Jan. 2010.

[22] P.Y. Liegeois, F. Leynaert, F. Meibody-Tabar, S. Pierfederici, and B. Nahid-Mobarakeh. "Electric actuator including two current-controlled voltage inverters powering an electric machine, and reconfigurable in the presence of a defect," WIPO Patent WO/2010/034906, Apr. 1, 2010.

[23] W. Zhao, K.T. Chau, M. Cheng J. Ji, and X. Zhu, "Remedial Brushless AC Operation of Fault-Tolerant Doubly Salient Permanent-Magnet Motor Drives," *IEEE Transactions on Industrial Electronics*, vol. 57(6), pp. 2134-2141, Jun. 2010.

[24] R.A. Hanna and S. Prabhu, "Medium-voltage adjustable speed drives-Users and manufacturers experiences," *IEEE Transactions on Industry Applications*, vol. 33(6), pp. 1407-1415, Nov./ Dec. 1997.